

Creep of Geopolymer and Alkali Activated Binder Concrete: Comparison with OPC Concrete and Design Codes

Han Gao¹, Iman Al-Damad², Ehab Hamed³, Ailar Hajimohammadi³ and Stephen Foster⁴

¹Doctoral student, Centre for Infrastructure Engineering and Safety, UNSW Sydney, Australia

²Research Associate, Centre for Infrastructure Engineering and Safety, UNSW Sydney, Australia

³Associate Professor, Centre for Infrastructure Engineering and Safety, UNSW Sydney, Australia

⁴Professor and Dean, Faculty of Engineering, UNSW Sydney, Australia

Abstract: Australia, alongside more than 110 countries, aims to achieve net zero greenhouse gas emissions by 2050. While progress has been made in defining the energy pathway, limited work has been done for low-emissions binders in the industrial sector, particularly in concrete. Geopolymer and alkali activator binder concretes have become viable alternatives to ordinary Portland cement (OPC) concrete in Australia. However, their long-term effects like creep and shrinkage are less understood. This paper discusses the creep model presented in the Standards Australia Technical Specification 199 (SA TS 199:2023) and provides experimental results for ambient-cured geopolymer concrete compared to traditional concrete. Existing prediction models are used to forecast geopolymer concrete's creep behaviour. It demonstrates that design codes for OPC concrete cannot be applied to geopolymer mix in this study, but the SA TS 199 provides accurate predictions for the tested design mix.

Keywords: Creep, geopolymer, alkali activated materials, prediction models, concrete.

1. Introduction

Extensive research has been carried out on geopolymer (GP) and alkali activated binders (AAB) as potential alternatives to ordinary Portland cement (OPC) as the binder for concrete. However, the long-term structural properties, specifically creep and shrinkage, have not been thoroughly demonstrated. This knowledge gap can be attributed to the inherent differences in micro and atomic structures between alkali activated binder concrete (AABC) and ordinary Portland cement concrete (OPCC). Despite the promising potential of these alternative binders, further investigation is needed to better understand and predict their long-term behaviour.

Wallah [1] investigated the drying creep behaviour of fly ash based Geopolymer concrete (GPC) and compared their obtained creep results with those of OPCC of similar compressive strength measured by other authors. Their study showed that creep of heat cured fly ash based geopolymer concrete is less than that of OPCC, with final creep coefficient of their mix and curing conditions of the order of 50% lower than the value predicted by using models proposed in AS 3600:2018 [2]. Sagoe-Crentsil et al. [3] conducted creep experiments on both fly-ash based geopolymer concrete and OPC concrete of equivalent grade to study the differences in creep between these two types of concrete. The results showed creep of fly ash based geopolymer concrete of 40-60% lower than that of the compared OPCC after 1 year of testing. Contrary to the observation of creep of fly ash based geopolymer concrete reported by the two authors, Un [4] found that slag-based alkali activated concrete synthesised with almost 100% slag exhibited much higher creep as opposed to that of OPCC.

This paper outlines the background to the creep model presented in SA TS 199:2023 [5] and reports on creep development of an ambient cured slag and fly ash blended alkali activated concrete and comparison to its prediction using the SA approach. The paper also presents on the qualifying the coefficients needed that adjust the model for element thickness and environment.

2. Background to the development of SA TS 199:2023 creep model

In reviewing the creep data available for GP and AAB concrete, extending over periods of one to four years, it was observed, unlike that of OPCC, that when the creep coefficient is plotted against the log of time, no signs of curtailment with increasing log-time is evident. An example of this is presented in Figure 1 for specimen GPC121113-14d of Un [4], loaded at day 14 and tested over 1200 days. This observation is not new, Hanson [6] and Harboe [7] proposed a logarithmic law for concrete creep. In a similar vein, to Bazant and Chern [8] it became apparent that the final slopes of long-term creep curves, as predicted by the double-power law, tend to be consistently higher than supported by the data. To address this, a transition to a

straight line on the logarithmic scale of load duration was introduced, resulting in a more accurate representation of the observed creep behavior.

Similar to that observed in [8], in observations across different testing series for GPC, a common creep-time form is observed when creep is plotted against the log of time: (1) there is a gradual acceleration of creep with log-time to a transition point (t_c); and (2), beyond t_c the rate of change creep strain is approximately constant with increasing log-time.

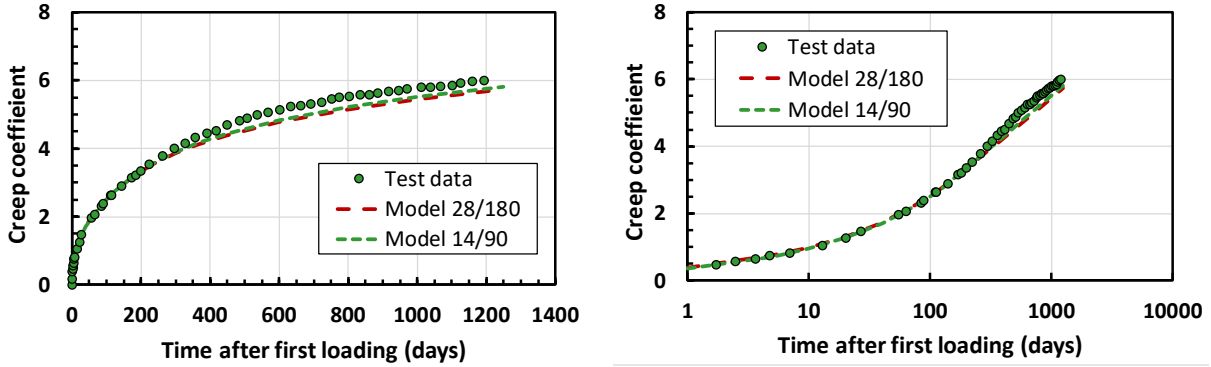


Figure 1. Creep coefficient versus time (left) and log-time (right) for mix GPC121113-14d of [4]

Prior to the point of transition, a simple exponential function is utilised:

$$\text{For } 1 \leq t \leq t_c \text{ days: } \varphi_{cc}(t) = at^b \quad (1)$$

At the transition point, the slope is calculated as:

$$\text{slope} = \left[\frac{d}{dt} (at_c^b) \right] / \left[\frac{d}{dt} (\ln t) \right] = abt_c^b \quad (2)$$

and thus:

$$\text{For } t > t_c \text{ days: } \varphi_{cc}(t) = at_c^b + abt_c^b [\ln(t) - \ln(t_c)] \quad (3)$$

where t is time in days after loading, $\varphi_{cc}(t)$ is the design creep coefficient at time t , t_c is time at transition and a and b are fitting parameters. The model is depicted in Figure 2.

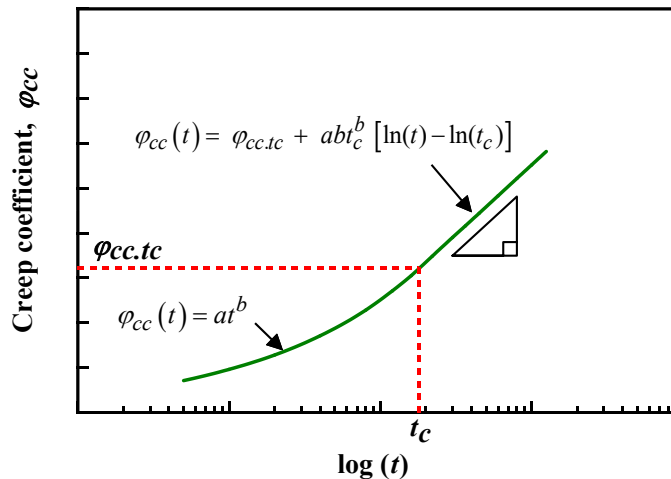


Figure 2. Model depicting creep coefficient versus log-time for GPC and AABC [5]

In a performance-based specification, parameters a and b may be determined from test data on the mix design being certified by picking any two points sufficiently distant apart – in examining the function, the first should not be before day 14 after the application of first loading.

Solving Eq. (1) and with t_1 and t_2 taken as not greater than t_c , we obtain:

$$a = \frac{\varphi_{cc}(t_1)}{t_1^b} = \frac{\varphi_{cc}(t_2)}{t_2^b} \quad \dots \quad b = \ln\left(\frac{\varphi_{cc}(t_2)}{\varphi_{cc}(t_1)}\right) / [\ln(t_2/t_1)] \quad (4)$$

where t_1 and t_2 are time after loading (in days). The expression of creep strains (ε_{cc}) or specific creep can be approached in a similar manner as the creep coefficient. In this case, the substitution of $\varphi_{cc}(t)$ with ε_{cc} or specific creep in Eqs. (1)–(4) is made, depending on the context, while considering that the values of a and b are determined based on the chosen measure.

For cases where $t_1 \leq t_c < t_2$, Eqs. (1) and (3) give:

$$a = \frac{\varphi_{cc}(t_1)}{t_1^b} \quad (5)$$

$$f = \frac{\varphi_{cc}(t_1)}{\varphi_{cc}(t_2)} = \frac{t_1^b}{t_c^b (1 + b \cdot l_{2,c})} \quad (6)$$

where $l_{2,c} = \ln(t_2) - \ln(t_c)$. Eq. (6) may be solved numerically to find b and then substituted into Eq. (5) for a .

In review of the model predictions against all data available for GPC and AABC, $t_1 = 14$ days and $t_2 = 90$ days provides good predictions in most cases and t_c taken as 180 days or determined from the data. Where higher confidence is needed for critical infrastructure, SA TS 199:2023 [5] recommends at least 180 days of creep data, in which case, $t_1 = 28$ days and $t_2 = t_c = 180$ days is found to provide a good predictive model. Figure 1 demonstrates the model predictions for mix GPC121113-14d of [4] for t_1/t_2 equal to 14/90, and 28/180; the transition time is taken as $t_c = 180$ days. For model 14/90, $a = 0.364$ and $b = 0.419$; whereas, for 28/180 $a = 0.386$ and $b = 0.407$. A good correlation between the models and long-term test results is observed.

For buildings designed for a 50-year life, the final creep coefficient ($t = 18,000$ days) obtained from Eq. (3) is:

$$\varphi_{cc}^* = at_c^b (1 + b [\ln(18,000) - \ln(t_c)]) \quad (7)$$

where a and b are determined from the values of φ_{cc} at the selected sampling times, t_1 and t_2 . For $t_c = 180$ days, Eq. (7) simplifies to:

$$\varphi_{cc}^* = a180^b (1 + 4.6b) \quad (8)$$

The final creep strain may also be determined from Eqs. (7) and (8) by replacing φ_{cc}^* with ε_{cc}^* and determining a and b from the creep strains (ε_{cc}) taken at t_1 and t_2 .

3. Comparison of SA TS 199:2023 Creep Model for AAB and OPC Concretes

In this Section, several applications of the model described above and adopted by SA TS 199:2023 [5] are compared – examples include AABC as well as OPCC.

In the first example, the data of Titus et al. [9] is re-examined. In this study data was collected for a 139 MPa mean compressive strength mix with partial cement replacement with 40% of activated slag. The results of the analysis are shown in Figure 3. Also compared are the predictions based on the AS3600 model calibrated using the method outlined in [10], with model calibration taken at times $t = 90$ and 365 days. The SA TS 199 model is calibrated for $t_1 = 14$ days, $t_2 = 90$ days (denoted as 14/90) and $t_c = 180$ days. With the first 90 days of data, and from Eq. (4), $a = 0.172$, $b = 0.257$.

The analysis reveals that the test calibrated AS3600 model (see [10]) significantly underestimates the long-term creep coefficient and, thus, creep strain, giving a final creep coefficient of 1.06 when tuned to the 365-day point, but just 0.85 when tuned using the 90-day point. The difference in these predictions demonstrated

the flaw in this approach where the form of the model does not follow that of the available data (see [10]) for a 50-year loading duration, while the 14/90 model, defined by Eq. (5) or (6), results in a 50-year creep coefficient of $\varphi_{cc}^* = 1.43$, an increase of 35 to 75%, depending on the tuned model point selected in the approach of [10].

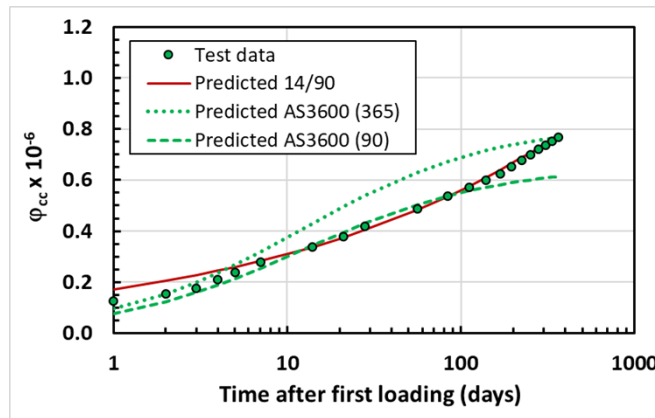


Figure 3. Comparison of SA TS 199:2023 and AS 3600:2018 models for AABC mix of [8]

For the second example, the 12-year creep data for OPCC of Taerwe [11] is examined. The mix consisted of 1060 kg of 8/16 siliceous river gravel, 190 kg of 4/8 siliceous river gravel, 100 kg of 2/5 river sand, 535 kg of 0/2 river sand, 360 kg of OPC (CEM 1-40) and 165 kg off water. The water to cement ratio was 0.46. The tests consisted of axially loaded prismatic specimens of 140 mm by 150 mm in cross-section and 4.0 m length. Loads were applied using unbonded prestressed stands that were regularly re-tensioned to maintain the load to within +/- 2%. In their tests, three sustained stress levels were investigated, concrete stresses σ_c of 5, 10 and 15 MPa, representing sustained stresses of 11, 21 and 32% of the concrete's 28-day cube compressive strength of 47.4 MPa (equivalent to 12, 25 and 37% of cylinder strength, respectively). In viewing the data, the transition time was taken as 28 days and the parameters b and a determined from Eqs. (6) and (5), respectively.

Figure 4 presents the results of the analyses conducted on the Taerwe data. It is observed that the creep is reasonably predicted by the SA TS199 model [5], with a calibration time of $t_c = 28$ days. The AS3600:2018 model (refer to [10]), tuned at $t = 365$ days, performs well in predicting the final creep strain but is less accurate at earlier ages. It is worth noting that the AS3600 model exhibits an earlier and more pronounced flattening compared to the data, where it is observed that continued logarithmic creep occurs beyond year 12 after the application of the load.

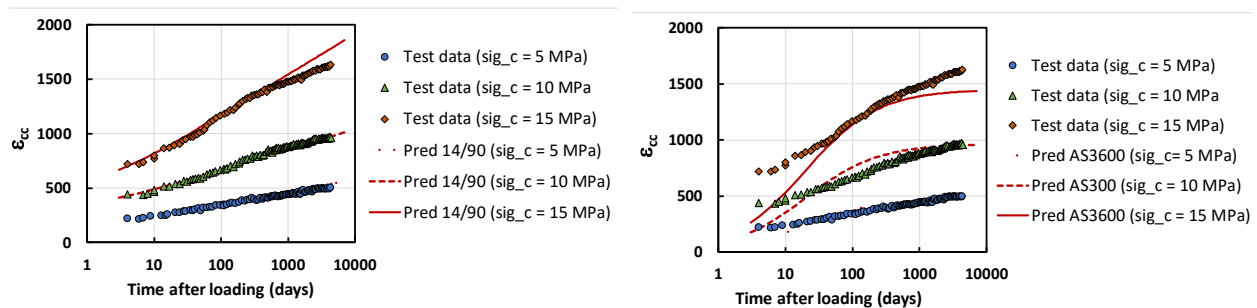


Figure 4. Comparison of SA TS 199 (left) and AS 3600 (right) models for OPCC mix of [10]

In this final example, the results of the OPCC mix design of Khatri and Sirivatnanon [12] are examined. This paper reported on testing carried out in CSIRO over a period of 11 years. The concrete mix examined was reported to contain GP cement and Basalt aggregate from NSW.

Figure 5 compares the results of the model presented above with $t_c = 180$ days, together with the method outlined in Supplement 1 to AS3600:2018 [10] with model calibration $t = 365$ days. It is observed that the specific creep results have not shown flattening as anticipated by the model but, rather, continue logarithmic creep for at least 11 years. The SA TS 199 14/90 model shows good correlation to the test data.

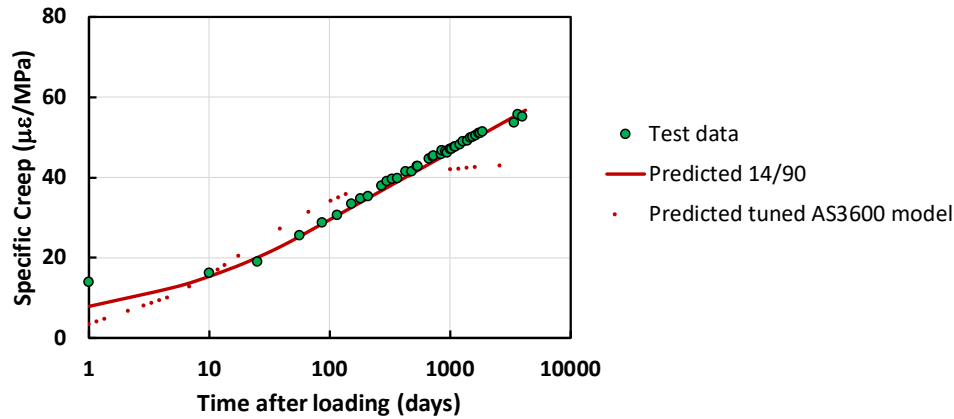


Figure 5. Comparison of SA TS 199 and data tuned AS 3600 models for OPCC mix of [12]

4. Influence of environment on creep

According to [5], the design creep coefficient (φ_{cc}) for a GPC and AABC at time, t , may be determined from the basic creep ($\varphi_{cc,b}$), which are calibrated such that $\varphi_{cc,b}$ is also predicted by the chosen model. In the absence of more accurate methods, φ_{cc} at any time t may be calculated from:

$$\varphi_{cc} = c_2 c_3 c_4 \varphi_{cc,b} \quad (7)$$

where c_2 is a factor dependent of the hypothetical thickness of the element relative to that of the creep test undertaken; c_3 is a factor dependent of the concrete's age at the time of first loading; and c_4 a factor to account for variation of environmental conditions to that of the creep test.

To demonstrate the approach, two arrangements of creep testing were undertaken for an AABC mix design developed as a part of a larger study. The precursor materials for the AABC consisted of 19 kg of ground granulated blast furnace slag (GGBFS) and 6.3 kg Class F Eraring fly ash. Solid sodium metasilicate anhydrous activator was used to activate the reaction, with molar ratio ($\text{SiO}_2/\text{Na}_2\text{O}$) = 0.91. The activator was mixed directly with the binder material and had a mass of binder to solids of 12.5%. Blue metal (51.8kg) and basalt (22.2 kg) were used as coarse aggregates and River Sand (40.9 kg) and Sydney Sand (17.2 kg) used as fine aggregate. All the aggregates were in saturated surface dry conditions before casting. After dry mixing for 2 minutes, 12.4 litres of water was added for a water to binder ratio of 0.49. Wet mixing continued for a further 10 minutes before casting of the specimens. The slump immediately after mixing was measured as 170 mm.

Cylindrical specimens of 100 mm diameter and 200 mm high were cast using steel moulds. All specimens were demoulded after 1 day and sealed with plastic wrap to prevent moisture loss for the next 6 days, as per the recommendations of [5], and placed in an environmental room set up at 23 °C and 50% relative humidity. After 6 days, the plastic wrapping was removed from one half of the samples (to measure total creep), while maintained on the other one-half (to measure creep of sealed specimens) and kept in the environmental room until day 28 after casting. The 28-day cylinder compressive strength of the concrete was determined in accordance with AS1012.9 [13] as $f_{cm} = 43$ MPa. The elastic modulus was measured at 28 days as $E_c = 31.2$ GPa, in accordance with AS1012.17 [14].

At 28 days after casting, creep tests were set-up in accordance with AS1012.16 [15], using a spring-supported loading frame. In each rig, three concrete specimens were stacked atop one another with a half-cylinder at each end. To monitor the strain over time, each specimen was attached with three Demec gauge targets on each of the three cylinders as well as two electrical strain gauges on the surfaces of each cylinder. Average values were derived from the measurements acquired from the five gauges on each cylinder and then further averaged over the three cylinders.

In addition to the creep tests, three control samples were prepared to measure the shrinkage strain, which was subtracted from the total strains to obtain the creep strains. Both basic creep and drying creep were measured. To measure basic creep, the cylindrical specimens were sealed with several layers of plastic wrap, followed by several layers of aluminium foil to prevent any loss of moisture over the testing period. The creep specimens were loaded through a hydraulic jack and spring system with a force of $P = 139$ kN, giving a stress 17.7 MPa ($\sigma_c/f_{cm} = 0.41$). The set-up for the creep tests is shown in Figure 6.



Figure 6. Creep testing of AABC (unsealed specimen left, sealed specimen right)

In Figure 7 the results of the sealed and unsealed creep tests are compared over a period of 400 days with t_c taken as 110 and 140 days for the unsealed and sealed specimens (as observed from the test data), respectively. According to the definition of AS3600:2018 [2], the basic creep coefficient is taken as the final creep coefficient determined for the case of a specimen with hypothetical thickness $t_h = 50$ mm (dia. = 100 mm), 50% relative humidity and loaded at a time of 28 days after casting at a stress ratio of 0.40. It is important to note here that the definition of basic creep in AS 3600:2018 differs to that of the international literature and standards. AS3600 is referring to a “basic” factor for creep calculations and not “basic creep” per se. To avoid confusion of practitioners using Australian standards, when referring to the basic creep coefficient in this paper, the AS3600 definition is used.

Taking the final time as 50 years, the determined basic creep coefficient for the mix presented above is $\varphi_{cc.b} = 5.83$. For the sealed specimens the determined final creep coefficient is $\varphi_{cc}^* = 4.15$ and, thus, c_2c_4 for this condition is $4.15/5.83 = 0.72$.

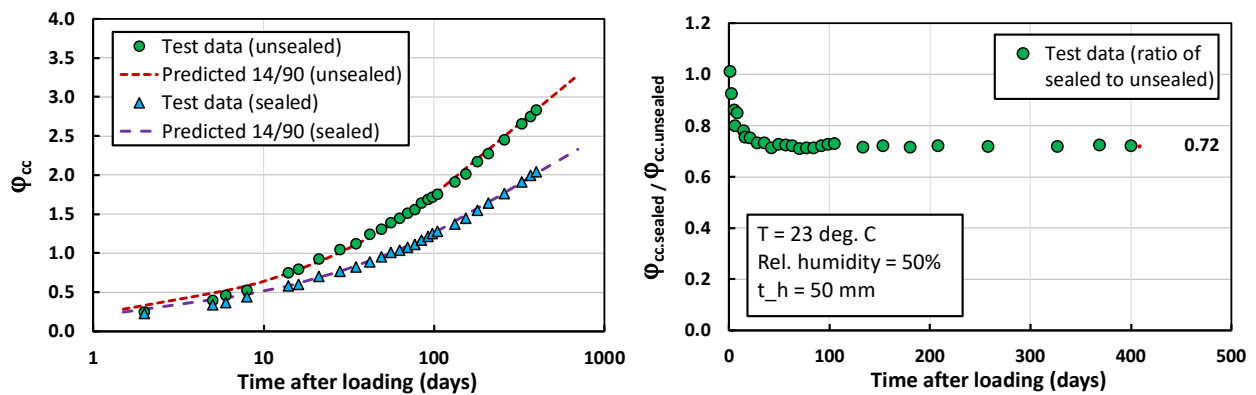


Figure 7. Comparison of creep in sealed and unsealed specimens (left) and calculation of c_4 (right).

For the case of the sealed specimen, which can be considered equivalent to an element of unlimited thickness at 100% humidity, the coefficients c_2c_4 holds a value of 0.72, which is higher than that prescribed for an OPCC mix according to [2], which for an element of $t_h = 400$ mm in a tropical would be give $c_2c_4 = 0.52$, and a for an arid environment 0.58. To delineate between the environmental component and the thickness component a third test is required, one of a different environmental condition, or of different thickness.

Assuming the effects of environment and thickness are maintained in the same proportion as that of OPCC then, according to the model of AS3600:2018, we might adjust each component by the ratio $0.72/0.58$

= 1.24. Thus, for this particular mix design: for arid environments (RH = 50%), a value of 0.85; for interior environments (RH = 60%), a value of 0.8; for temperate inland environments (RH = 65%), a value of 0.75; and for tropical, near-coastal, and coastal environments (RH = 70%), a value of 0.6. Taking the sealed condition as equivalent to a hypothetical thickness $t_h = 400$ mm and assuming a linear relationship for increasing t_h between 50 mm and 400 mm, the value for c_2 then becomes:

$$c_2 = 1.2 - 0.001(t_h - 50) \dots \text{within the limits } 0.85 \leq c_2 \leq 1.2 \quad (8)$$

The assumption of approximate linearity between t_h of 50 and 400 mm can be readily tested through testing of one or several intermediate thicknesses under identical environmental conditions. While the model for this mix might be considered as sufficiently accurate within the error bounds of the AS3600:2018 creep model for concrete structures of +/- 30%, nevertheless, to gain a more comprehensive understanding of the behavior of this mix across a wider range of thicknesses and environmental conditions, additional tests should be conducted.

5. Conclusions

Geopolymer and alkali activator binder concretes are rapidly gaining recognition as viable alternatives to conventional ordinary Portland cement (OPC) concrete in Australia, offering the potential to significantly reduce CO₂-eq emissions associated with concrete production. However, the long-term behaviour of these innovative concretes, particularly in relation to creep and shrinkage, remains relatively unexplored.

This paper provides a comprehensive overview of the background and development of the model presented in the Standards Australia Technical Specification 199 (SA TS 199:2023). Through a comparative analysis of experimental tests conducted on ambient-cured geopolymer and alkali activator binder concretes, alongside traditional OPC concrete, the study investigates the crucial aspects of in development of models for design of concrete structures for creep. These parameters play a vital role in the design and construction processes, enabling engineers to effectively utilise these novel concretes in practice.

The findings of this research underscore the inapplicability of design model codes developed for OPC concrete to non-traditional binder concretes. The study confirms that the SA TS 199 model provides accurate predictions for the tested design mixes, demonstrating its reliability and suitability as a valuable tool for engineers, an demonstrates calibration of the model for environmental, thickness and time of loading parameters. The model also exhibits strong performance when compared against long-term data collected for OPC concrete, especially in scenarios where a calibration period of at least 90 days is undertaken and logarithmic growth behaviour is observed.

Importantly, while the SA TS 199 model was specifically developed for geopolymer and alkali activator binder concretes, its underlying approach, which utilises a data-tuned methodology, holds applicability for other new binder concretes that display logarithmic creep behaviour. Lastly, the study validates the suitability of the SA TS 199 model for predicting creep and underscores its applicability for future alternative binder concrete currently in development that display logarithmic creep characteristics.

6. References

1. Wallah, S.E., Creep behaviour of fly ash-based geopolymer concrete. *Civil Engineering Dimension*, Vol. 12, No. 2, 2010, pp. 73-78.
2. AS 3600:2018, *Concrete Structures*, Standards Australia, Sydney, 2018, 268 pp.
3. Sagoe-Crentsil, K., Brown, and Taylor, A., Drying shrinkage and creep performance of geopolymer concrete, *Journal of Sustainable Cement-Based Materials*, Vol. 2, No., 1, 2013, pp. 35-42.
4. Un, C.H., *Creep Behaviour of Geopolymer Concrete*, PhD Thesis, Faculty of Science, Engineering and Technology, Swinburne University of Technology, Melbourne, Australia, 2017, 282 pp.
5. SA TS 199:2023, *Design of geopolymer and alkali-activated binder concrete structures*, Standards Australia, Sydney, Australia, 2023, 101 pp.
6. Harboe, E., A comparison of the instantaneous and the sustained modulus of elasticity of concrete, in *Concrete Laboratory Report 1958*, US Bureau of Reclamation, Denver Colorado, USA.

7. Hanson, J.A., A Ten-Year Study of Creep Properties of Concrete in Concrete Laboratory Report. 1953, US Bureau of Reclamation, Denver Colorado, USA, 34 pp.
8. Bažant, Z.P., and Chern, J-C, Research, Double-power logarithmic law for concrete creep, Cement and Concrete Research, Vol. 14, No. 6, 1984, pp. 793-806.
- 9 Titus, H., Tabone, M., Biondo, J., and Foster, S.J., Development of a high modulus, very high strength, high performance, super-workable low carbon concrete, Better, Smarter, Stronger Proceedings for the 2018 fib Congress (Eds. Foster, S. et al.), 7-11 October, Melbourne, Australia, 2019, Fédération Internationale du Béton (fib), Lausanne, Switzerland, pp. 3936–3944.
- 10 AS 3600:2018 Sup 1:2022, Concrete structures – Commentary (Supplement 1 to AS 2300:2018), Standards Australia, Sydney, Australia, 2022, 305 pp.
11. Taerwe, L.R., Influence of passive reinforcement on creep and shrinkage of concrete: long-term observations, Presentation to CEOS International Workshop, 10-11 December, 2009, Paris, France, 38 pp.
12. Khatri, R., and Sirivivatnanon, V., Long term behaviour of concrete: creep and shrinkage, CIA Presentation, Sydney, 2006, 11 pp.
13. AS 1012.9:2014, Methods of testing concrete, Method 9: Compressive strength tests – concrete, mortar and grout specimens, Standards Australia, Sydney, Australia, 2014, 12 pp.
14. AS 1012.17:1997, Methods of testing concrete, Method 17: Determination of the static chord modulus of elasticity and Poisson's ratio of concrete specimens, Standards Australia, Sydney, Australia, 1997, 16 pp.
15. AS 1012.16:1996, Methods of testing concrete, Method 16: Determination of creep of concrete cylinders in compression, Standards Australia, Sydney, Australia, 1996, 8 pp.